Advances in Radio Science, 3, 199–204, 2005
SRef-ID: 1684-9973/ars/2005-3-199

Advances in Radio Science

Exponential Modelling for Mutual-Cohering of Subband Radar Data

U. Siart, S. Tejero, and J. Detlefsen

Institute for High-Frequency Engineering, Technische Universität, Arcisstr. 1, 80333 München, Germany

Abstract. Increasing resolution and accuracy is an important issue in almost any type of radar sensor application. However, both resolution and accuracy are strongly related to the available signal bandwidth and energy that can be used. Nowadays, often several sensors operating in different frequency bands become available on a sensor platform. It is an attractive goal to use the potential of advanced signal modelling and optimization procedures by making proper use of information stemming from different frequency bands at the RF signal level. An important prerequisite for optimal use of signal energy is coherence between all contributing sensors. Coherent multi-sensor platforms are greatly expensive and are thus not available in general. This paper presents an approach for accurately estimating object radar responses using subband measurements at different RF frequencies. An exponential model approach allows to compensate for the lack of mutual coherence between independently operating sensors. Mutual coherence is recovered from the *a-priori* information that both sensors have common scattering centers in view. Minimizing the total squared deviation between measured data and a full-range exponential signal model leads to more accurate pole angles and pole magnitudes compared to single-band optimization. The model parameters (range and magnitude of point scatterers) after this full-range optimization process are also more accurate than the parameters obtained from a commonly used super-resolution procedure (root-MUSIC) applied to the non-coherent subband data.

1 Introduction

It is well known that the fundamental limit for radar range resolution is the signal bandwidth, provided there is no additional limitation through noise. Classical radar signal theory (see Cook and Bernfeld, 1993, for a comprehensive overview) relates range resolution to the effective bandwidth of the radar transmit signal. Super-resolution methods like autoregressive modelling (AR) or eigenanalysis methods (e.g. MUSIC) can achieve better resolution compared to the classical limits. They are basically model-based parameter estimators that use prior knowledge about the signal. Their performance and properties have been exhaustively investigated in the past (Pesavento et al., 2000; Zhang, 1998; Rao and Hari, 1989; Marple, 1987) just to mention a few).

In recent times and even more in the future there will be sensor platforms with not only one but several radar sensors designed for various purposes. Automotive radar equipment for parking aid, adaptive cruise control and a variety of driver assistance and comfort functions is an example from the low-cost sector. Also nowadays there are remote sensing platforms that gather information with more than one radar system. This rises the question for making optimum use of information that comes from different radar sensors and in different frequency areas. A prerequisite for optimum processing of multi-band radar information would be mutual coherency between the sensors in order to utilize also mutual phase information. For expenditure reasons, individual sensors on a platform are most often mutually incoherent so this condition is normally not fulfilled.

The purpose of this work is to investigate signal processing methods to restore coherency between the data from mutually incoherent radar sensors. The approach is different to sensor fusion techniques. It attempts to merge radar sensor information directly on the raw radar data level while sensor fusion techniques apply to fully processed sensor data for the sake of a more convenient object classification or multi-static radar measurements (e.g. Meinecke et al., 2003; Schiementz et al., 2003; Thomopoulos and Okello, 1993).

An important assumption behind the published approach is that the contributing sensors bring information about the same scenery. In a first approach, it is further assumed that the common scenery is observed from the same direction by two sensors as depicted in Fig. 1. The sensors generally operate at different carrier frequencies and with different signal bandwidths.

It is further assumed that the radar scenery is well approximated by an ensemble of real or effective discrete scattering centers and that the same scatterers are active in both sensors' frequency regimes. As a consequence, the radar response is considered to be mainly a multi-path response including P paths with identical round trip times τ_p in both sensors. Let us also assume that the radar data is given in frequency

Correspondence to: U. Siart
(uwe.siart@tum.de)

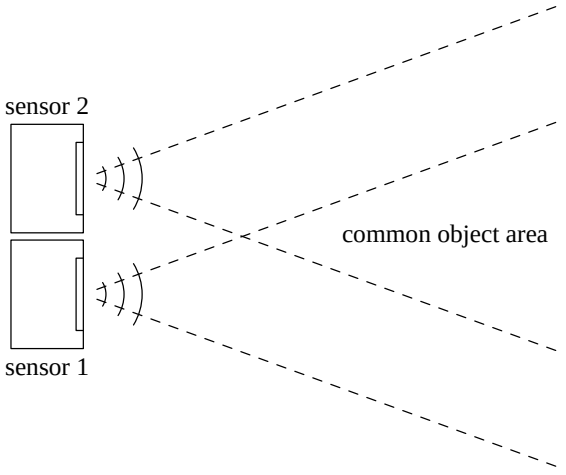

Fig. 1. Dual-band radar sensing of a common object area.

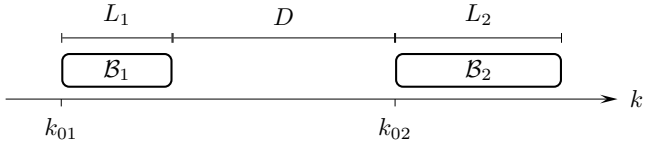

Fig. 2. Illustration of the parameters used to specify bandwidth and band gap.

domain. Both sensors deliver a discrete-frequency measure of the complex reflectivity, using the same angular frequency increment $\Delta\omega$. If the bandwidth of frequency band $\mathcal{B}_{1,2}$ is $B_{1,2}$, then the length of the data sequence is $L_{1,2}{=}B_{1,2}/\Delta\omega$, respectively. The distance in between bands $\mathcal{B}_1$ and $\mathcal{B}_2$ is also given in terms of angular frequency increments D. The start index of each band is $k_{01,2}{=}+{-}\omega_{01,2}/\Delta\omega$ where $\Delta\omega_{01,2}$ are the lower angular frequencies of each band. See Fig. 2 for illustration.

With these assumptions, the discrete-frequency complex reflectivity is

$$r[k] = \sum_{p=1}^{P} A_p \cdot e^{-j\Omega_p k} \tag{1}$$

where $\Omega_p{=}\Delta\omega{\cdot}\tau_p$ and $k{=}\omega/\Delta\omega$. If Eq. 1 is measured by a radar system no. n with angular frequency increment $\Delta\omega$, starting from the lower frequency ω_{0n}, and with bandwidth $B_n{=}L_n{\cdot}\Delta\omega$, then the noiseless data from this sensor is

$$r_n[k] = \sum_{p=1}^{P} A_p {z_p}^{k+k_{0n}} = \sum_{p=1}^{P} a_{pn} {z_p}^{k} \tag{2}$$

with $k = 0, 1, \ldots, L_n{-}1$. In this notation $z_p{=}e^{-j\Omega_p}$ and $a_{pn}{=}A_p e^{-j\omega_{0n}\tau_p}{=}A_p {z_p}^{k_{0n}}$. If the measurements are mutually coherent and Eq. 1 is valid in frequency bands $\mathcal{B}_1$ and $\mathcal{B}_2$, then necessarily

$$\frac{a_{p2}}{a_{p1}} = e^{-j\Omega_p(k_{02}-k_{01})}\,. \tag{3}$$

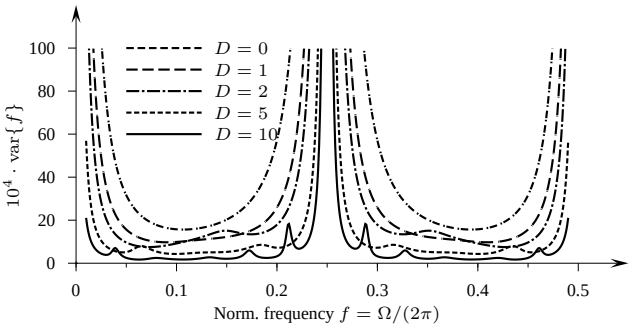

Fig. 3. Cramér-Rao lower bound for dual-band dual-frequency estimation.

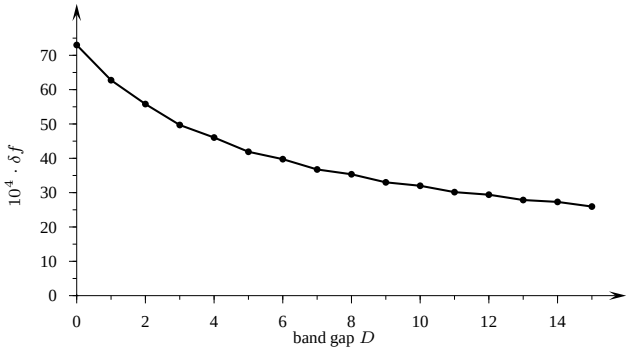

Fig. 4. Maximum achievable resolution versus band gap.

Equation 3 can be considered as the condition for mutual coherence between the data in $\mathcal{B}_1$ and $\mathcal{B}_2$.

2 Cramér-Rao lower bound

Estimating the range parameter of point scatterers observed by a radar system can be considered equivalent to estimating the frequency of a real or complex sinusoid in the frequency response of the radar scenery. With frequency modulated continuous wave (FMCW) or stepped-frequency radar this is task naturally appears. But the information delivered by any arbitrary impulse response measurement technique can in principal be processed in the frequency domain, where the round trip time of discrete echos corresponds to the frequencies of sinusoids. To investigate the maximum achievable resolution through dual-band estimation, the Cramér-Rao lower bound (CRLB) for frequency estimation of a sinusoid from dual-band data under the presence of a second sinusoid with equal magnitude is derived. It is assumed that the observed discrete data from bands $\mathcal{B}_{1,2}$ have the form

$$x_{1,2}[k] = s_{1,2}[k, \boldsymbol{\theta}] + w_{1,2}[k] \tag{4}$$

where the noiseless signals are

$$s_1[k, \boldsymbol{\theta}]{=}A\cos(2\pi f_1 k{+}\phi_1) \; {+}A\cos(2\pi f_2 k{+}\phi_2) \tag{5a}$$
$$s_2[k, \boldsymbol{\theta}]{=}A\cos(2\pi f_1 k{+}\phi_{12}){+}A\cos(2\pi f_2 k{+}\phi_{22}) \tag{5b}$$

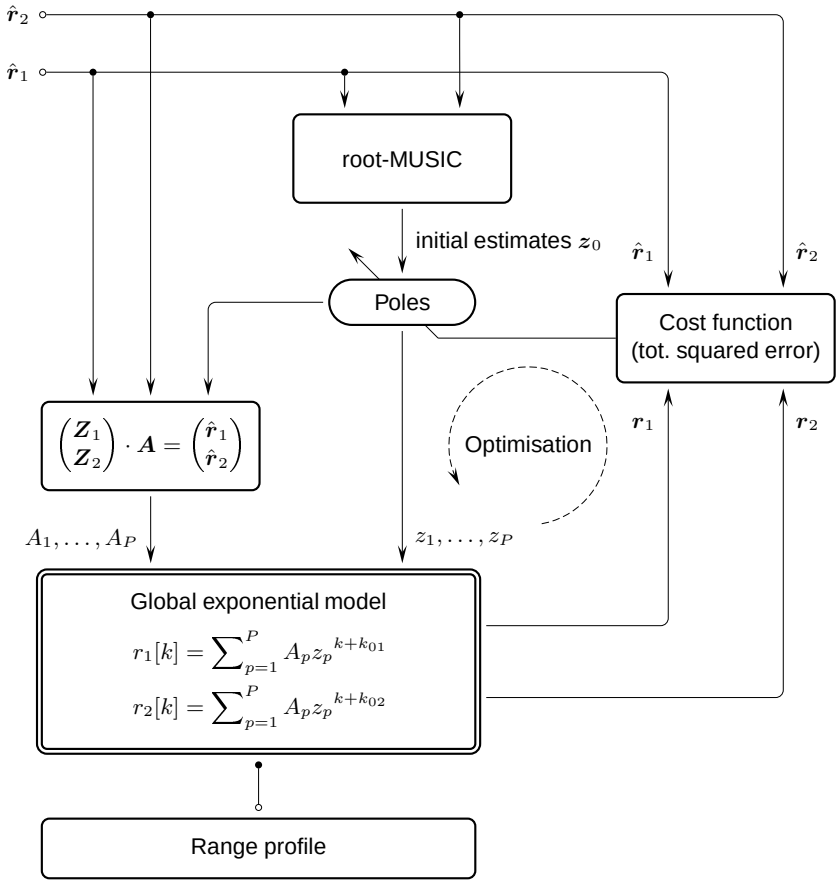

Fig. 5. Block diagram of the proposed global model fitting procedure.

and $w_{1,2}[k]$ is white Gaussian noise. Coherency between the bands implies that

$$\phi_{12} = \phi_1 - 2\pi f_1(L_1 + D) \tag{6a}$$

$$\phi_{22} = \phi_2 - 2\pi f_2(L_1 + D) \tag{6b}$$

and the parameter vector is $\boldsymbol{\theta}=[f_1\ f_2\ \phi_1\ \phi_2]^{\mathrm{T}}$. Assuming that the noise is white and Gaussian, the Fisher information matrix following Kay (1993) is

$$[\boldsymbol{I}(\boldsymbol{\theta})]_{ij} = \frac{1}{\sigma^2}\left(\sum_{\mathcal{B}_1}\frac{\partial s_1[k,\boldsymbol{\theta}]}{\partial\theta_i}\cdot\frac{\partial s_1[k,\boldsymbol{\theta}]}{\partial\theta_j}+\sum_{\mathcal{B}_2}\frac{\partial s_2[k,\boldsymbol{\theta}]}{\partial\theta_i}\cdot\frac{\partial s_2[k,\boldsymbol{\theta}]}{\partial\theta_j}\right). \tag{7}$$

From this, the CRLB for the i-th parameter is

$$\mathrm{var}(\theta_i) \geq [\boldsymbol{I}^{-1}(\boldsymbol{\theta})]_{ii}\,. \tag{8}$$

A plot of $[\boldsymbol{I}^{-1}(\boldsymbol{\theta})]_{ii}$ under the presumption that f_2=0.25 and ϕ_1=ϕ_2=0 is shown in Fig. 3. In this figure the distance D between the data windows varies while the window widths remain constant L_1=L_2=5. It is seen that estimation of frequency f_1 becomes inaccurate as f_1 approaches either DC or the Nyquist limit or if f_1 comes close to f_2. Furthermore it can be recognized that the increase of the CRLB nearby frequency f_2 is the slower, the wider the gap D.

Let us now define the minimum achievable resolution δf as the frequency difference $|f_2-f_1|$ where the CRLB of f_1 exceeds the difference $|f_2-f_1|$ that is to be resolved. Using this definition, the minimum resolvable frequency difference can be derived from Eq. 8 for any values of L_1, L_2, and D. As an example, the minimum achievable resolution (in this sense) is plotted in Fig. 4 versus the band gap D. In this figure, the length of the available data is L_1+L_2=20 and the signal-to-noise ratio is SNR=0 dB. The classical Rayleigh resolution limit Δ_{R} in this case is Δ_{R}=0.5/20=250·10^{-4}. It is seen that the resolution limit of an efficient estimator improves as the gap D between the frequency bands increases.

3 Model-based dual-band processing

Assuming that Eq. 1 is globally valid, then the signal model for the measured data $\hat{r}_{1,2}[k]$ in the subbands $\mathcal{B}_{1,2}$ is

$$r_1[k] = \sum_{p=1}^{P} A_p {z_p}^{k+k_{01}} \tag{9a}$$

$$r_2[k] = \sum_{p=1}^{P} A_p {z_p}^{k+k_{02}}\,. \tag{9b}$$

Table 1. Simulation parameters.

Quantity	*Value*
Length L_1 of subband 1	*32*
Length L_2 of subband 2	*32*
Number of complex sinusoids	*2*
Frequency difference	*variable*
Model order P	*one of 4/8*
Length D of interband gap	*one of 0/32/128*
Signal-to-noise ratio SNR	*variable*
no. of trials	*2 000*

This can be written in matrix notation

$$\boldsymbol{Z}\cdot\boldsymbol{A}=\begin{pmatrix}\boldsymbol{Z}_1\\ \boldsymbol{Z}_2\end{pmatrix}\cdot\boldsymbol{A}=\begin{pmatrix}\boldsymbol{r}_1\\ \boldsymbol{r}_2\end{pmatrix} \tag{10}$$

where $\boldsymbol{A}=[A_1,\ldots,A_P]^{\mathrm{T}}$, $\boldsymbol{r}_n=\big[r_n[0],\ldots,r_n[L_n-1]\big]^{\mathrm{T}}$ and

$$\boldsymbol{Z}_n=\begin{pmatrix} {z_n}^{k_{0n}+0} & {z_2}^{k_{0n}+0} & \cdots & {z_P}^{k_{0n}+0}\\ {z_n}^{k_{0n}+1} & {z_2}^{k_{0n}+1} & \cdots & {z_P}^{k_{0n}+1}\\ \vdots & \vdots & \ddots & \vdots\\ {z_n}^{k_{0n}+L_n-1} & {z_2}^{k_{0n}+L_n-1} & \cdots & {z_P}^{k_{0n}+L_n-1}\end{pmatrix}.$$

The purpose is to estimate the poles z_p under the boundary condition that the same values A_p apply to both subbands. Through $\tau_p=\Omega_p/\Delta\omega$ the pole angles Ω_p then yield the round trip times to be estimated. Generally, the amplitudes A_p may take any complex value and no prior knowledge is available about them. Given a set of poles z_p, optimum values A_p can be found by the least-squares solution of Eq. 10 when substituting $\boldsymbol{r}_{1,2}$ with the measured data $\hat{\boldsymbol{r}}_{1,2}$. With these parameters the signal model Eq. 9 is complete. As a measure for the modelling quality, the total square deviation

$$J=\sum_{\mathcal{B}_1}\big|\hat{r}_1[k]-r_1[k]\big|^2+\sum_{\mathcal{B}_2}\big|\hat{r}_2[k]-r_2[k]\big|^2 \tag{11}$$

between the signal model $\boldsymbol{r}_{1,2}$ and the measured data $\hat{\boldsymbol{r}}_{1,2}$ is used. This clarifies the exponential model fitting procedure under consideration. See Fig. 5 for a block diagram. A set of poles z_p forms the degrees of freedom while the corresponding amplitudes A_p follow from a least-squares comparison between P complex sinusoids with frequencies Ω_p and the measured data $\hat{\boldsymbol{r}}_{1,2}$. This global exponential model can be optimized iteratively by varying the pole angles.

Tuning the pole angles is a highly ambiguous problem, especially when the band gap D is large. Therefore it is required that the initial estimates for the pole angles are as accurate as possible. Super-resolution methods that are based on auto-covariance estimation are principally sufficient for processing mutually incoherent multi-band data. They do not employ mutual phase information even if the subband data were coherent, however. Phase information is introduced by the global signal model Eq. 1 that leads to the subband representation Eq. 2 and the phase condition Eq. 3.

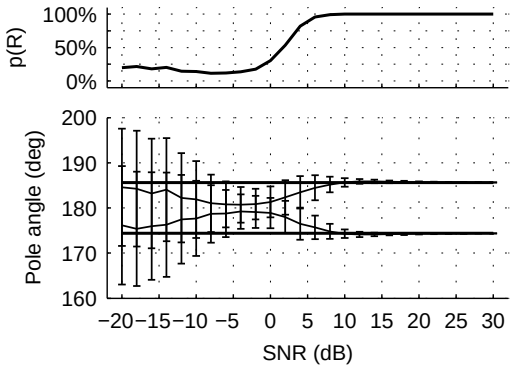

(a) $D=0$, $P=8$, $\Delta\Omega=2\Delta_{\mathrm{R}}$

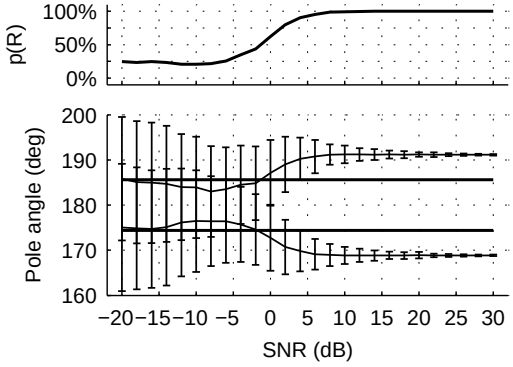

(b) $D=32$, $P=8$, $\Delta\Omega=2\Delta_{\mathrm{R}}$

Fig. 6. Resolution properties of an autoregressive model (covariance method).

In Fig. 5 the input measurement data is represented by the row vectors $\boldsymbol{r}_{1,2}$. To achieve initial estimates for the poles z_p the root-MUSIC algorithm is chosen. The according complex amplitudes A_p are determined by the minimum-least-squares solution of Eq. 10 where the measured data is substituted in the row vector on the right side. In the following the total squared deviation between the signal model and the measured data is minimized through an iterative nonlinear least-squares minimization algorithm based on the Levenberg-Marquardt method. During this optimization $|z_p|=1$ so the pole angles are the actual optimization parameters. In general, the difference $k_{02}-k_{01}$ is another degree of freedom when the data $\mathcal{B}_1$ and $\mathcal{B}_2$ are not coherent. It is used to set up the matrix $\boldsymbol{Z}$ in Eq. 10. In the following simulations it is assumed to be known, however. It should be noted that without any knowledge about the phase angles $\arg\{A_p\}$ only the difference $k_{02}-k_{01}$ can be estimated. The values $k_{01,2}$ are ambiguous because multiplication of $\boldsymbol{A}$ with $[{z_1}^m,\ldots,{z_p}^m]^{\mathrm{T}}$ in Eq. 10 with an arbitrary value m can always be compensated by adding $-m$ to all exponents in $\boldsymbol{Z}$.

Once the model parameters are optimized, the signal

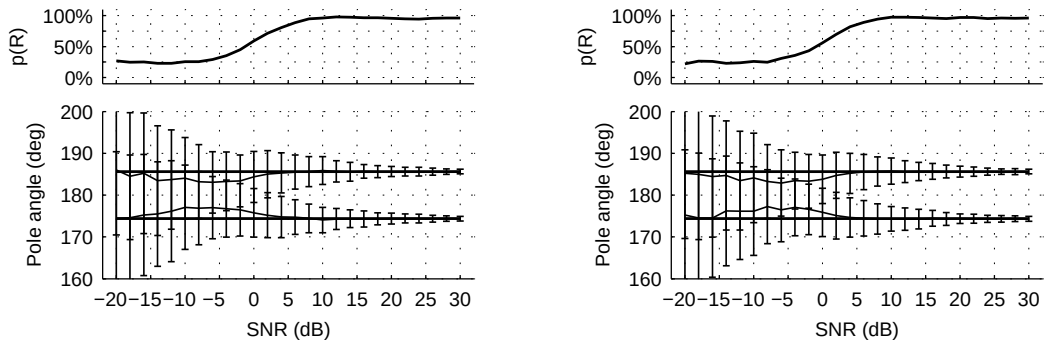

(a) $D = 0$, $P = 8$, $\Delta\Omega = 2\Delta_{\mathrm{R}}$ *(b)* $D = 32$, $P = 8$, $\Delta\Omega = 2\Delta_{\mathrm{R}}$

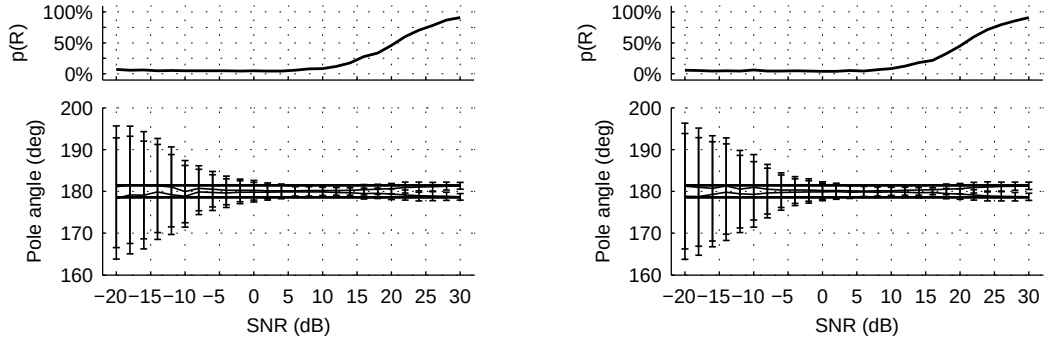

(c) $D = 0$, $P = 8$, $\Delta\Omega = 0.5\Delta_{\mathrm{R}}$ *(d)* $D = 32$, $P = 8$, $\Delta\Omega = 0.5\Delta_{\mathrm{R}}$

Fig. 7. Resolution properties of the root-MUSIC algorithm.

model can be used to compute the range profile. This can be done by either evaluating the pole angles directly or by using the model to compute an arbitrary number of interpolated and extrapolated samples along the frequency axis to achieve a closed data vector without any missing samples. Such a data series is then sufficient to provide a discrete Fourier transform (DFT) range profile. Although the signal model allows to extrapolate the measured data to any desired wide bandwidth, leading to arbitrary narrow pulses in the time/range domain, this bandwidth extrapolation yields neither additional information nor increased resolution. Radar pulses become narrow through bandwidth extrapolation but no additional targets or reflections will appear.

4 Simulation results

In the following simulations the mean and variance of pole angle estimates in the single-band and in the dual-band case are investigated. The length of the subband data is L_1=L_2=32 and the signal $s[k]$ consists of two complex sinusoids with equal magnitude. Their normalized frequency difference is given in comparison to the Rayleigh resolution bound Δ_{R}=$1/(L_1+L_2)$. The mean and variance estimates are based on 2000 trials and they are plotted versus the signal-to-noise ratio of the input data. A survey on the simulation parameter setup is given in Table 1.

From the resulting pole angle estimates the probability of resolution p(R) is computed. Since the total number of poles is given by the chosen model order, a criterion for proper detection and resolution of the targets based on the actual pole angles has to be introduced. The following procedure was used to plot p(R) in Figs. 6 to 8: Provided that Ω_i and Ω_j are the true pole angles to represent the two complex sinusoids then first find z_i of which arg$\{z_i\}$ is closest to Ω_i. Next find z_j of which arg$\{z_j\}$ is closest to Ω_j. The sinusoids are considered to be resolved if, and only if $|i-j|$=1.

Figure 6 shows the resolution properties and the quality of the pole angle estimates using an autoregressive (AR) model. This figure compares the single-band case (D=0, Fig. 6a to the dual-band case (D=32, Fig. 6b. The model order is P=8 and the frequency distance between the two sinusoids is twice the Rayleigh resolution bound. Resolution is achieved also in the dual-band situation but the estimates are biased, however. Therefore, AR estimation is not sufficient to provide accurate initial values for the exponential model optimizer although AR modelling can be applied to dual-band data.

As a comparison, the same approach using the root-MUSIC algorithm are shown in Fig. 7, additionally for the case where the frequency distance is only half the Rayleigh bound Δ_{R} (Figs. 7c, d. It is seen that the root-MUSIC result is not influenced by missing samples and that root-MUSIC

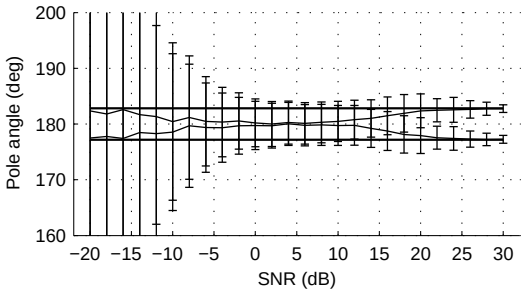

(a) $D = 0$, $P = 4$, $\Delta\Omega = \Delta_{\mathrm{R}}$

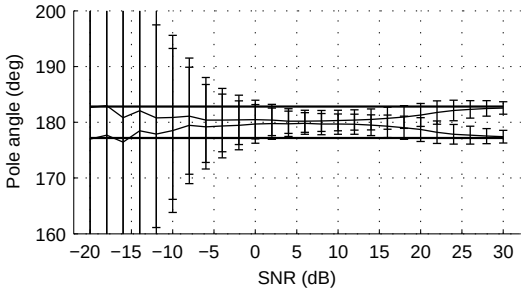

(b) $D = 128$, $P = 4$, $\Delta\Omega = \Delta_{\mathrm{R}}$

Fig. 8. Variance of the pole angle estimates after the global multiband model fit.

still achieves resolution below the Rayleigh bound, provided the signal-to-noise ratio is sufficiently high. For these properties, root-MUSIC was chosen as the initial pole angle estimator.

In Fig. 8 the statistical properties of the two poles closest to the true pole angles after the optimization procedure explained in section 3 are shown. The model order in this simulation is P=4 and the frequency distance is equal to the Rayleigh resolution bound. In Fig. 8a the optimization result using a single band (D=0) is shown in comparison to a dual-band optimized model in Fig. 8b. It is seen that in both cases the pole angle variance decreases considerably when SNR>22 dB. The variance also increases rapidly for SNR<0 dB. In the region 0 dB<SNR<22 dB the variance of the two poles closest to the true positions is considerably smaller when using dual-band data for the global model fitting procedure.

5 Conclusion

A model-based signal processing procedure for dual-band radar range estimation has been proposed. The algorithm basically recovers coherency between the distinct radar data by making use of the prior knowledge that identical scatterers form the radar range profile in both subbands. The Cramér-Rao lower bound indicates a smaller range estimation variance for the dual-band case compared to equal bandwidth single-band estimation, yielding a better resolution. A root-MUSIC algorithm is used to achieve initial range estimates from incoherent subband data. These initial estimates are further improved by making use of mutual phase information. This is achieved by fitting a global exponential model to the observed subband data and presuming that the exponential components are identical in both subbands. Simulation results show the improved accuracy of the coherent dual-band estimates compared to the result of conventional super-resolution methods.

References

Bresler, Y. and Macovski, A.: Exact Maximum Likelihood Parameter Estimation of Superimposed Exponential Signals in Noise, IEEE Trans. Acoust., Speech, Signal Processing, ASSP-34, 1081–1089, 1986.

Bruckstein, A. M., Shan, T.-J., and Kailath, T.: The Resolution of Overlapping Echos, IEEE Trans. Acoust., Speech, Signal Processing, ASSP-33, 1357–1367, 1985.

Chan, Y. T., Lavoie, J. M. M., and Plant, J. B.: A Parameter Estimation Approach to Estimation of Frequencies of Sinusoids, IEEE Trans. Acoust., Speech, Signal Processing, ASSP-29, 214–219, 1981.

Cook, C. E. and Bernfeld, M.: Radar Signals, An Introduction to Theory and Applications, Artech House, Boston, 1993.

Gu, H.: Estimating the Number of Signals and Signal Resolution, IEEE Trans. Signal Processing, SP-46, 2267–2270, 1998.

Kay, S. M.: Estimation Theory, vol. 1 of Fundamentals of Statistical Signal Processing, Prentice Hall, Upper Saddle River, 1993.

Kumaresan, R. and Tufts, D. W.: Estimating the Parameters of Exponentially Damped Sinusoids and Pole-Zero Modeling in Noise, IEEE Trans. Acoust., Speech, Signal Processing, ASSP-30, 833–840, 1982.

Liu, S. and Xiang, J.: Novel Method For Super-Resolution in Radar Range Domain, IEE Proc. Radar, Sonar and Navigation, Vol. 146, 40–44, 1999.

Marple, S. L.: Digital Spectral Analysis, Prentice Hall, Englewood Cliffs, 1987.

Meinecke, M.-M., Obojski, M. A., M., T., Dörfler, R., Marchal, P., Letellier, L., Dariu, G., and Morris, R.: Approach for Protection of Vulnerable Road Users Using Sensor Fusion Techniques, in: Proc. Int. Radar Symposium (IRS), DGON, Dresden, 125–130, 2003.

Pesavento, M., Gershman, A. B., and Haardt, M.: Unitary Root-MUSIC with a Real-Valued Eigendecomposition: A Theoretical and Experimental Performance Study, IEEE Trans. Signal Processing, SP-48, 1306–1314, 2000.

Rao, B. D. and Hari, K. V. S.: Performance Analysis of Root-MUSIC, IEEE Trans. Acoust., Speech, Signal Processing, ASSP-37, 1939–1949, 1989.

Schiementz, M., Fölster, F., and Rohling, H.: Angle Estimation Techniques for different 24 GHz Radar Networks, in: Proc. Int. Radar Symposium (IRS), DGON, Dresden, 405–410, 2003.

Thomopoulos, S. C. A. and Okello, N. N.: Design and experimental validation of a multiband radar data fusion system, in: Proc. SPIE, Boston, MA, 26–36, 1993.

Zhang, Q. T.: A Statistical Resolution Theory of the AR Method of Spectral Analysis, IEEE Trans. Signal Processing, SP-46, 2757–2766, 1998.